Ultrasonic and microwave investigation of the structural and magnetic transitions in $CaFe_2As_2$ and $BaFe_2As_2$ single crystals

Mario Poirier, Maxime Bilodeau, and Simon Lefebvre
Regroupement Québécois sur les Matériaux de Pointe, Département de Physique, Université de Sherbrooke, Sherbrooke, Québec, Canada J1K 2R1

Amar B. Karki and Rongying Jin
Department of Physics and Astronomy, Louisiana State University, Baton Rouge, Louisiana 70803, USA
(Received 25 February 2014; revised manuscript received 7 April 2014; published 22 April 2014)

Pulsed ultrasonic experiments performed on the parent compounds of FeAs based superconductors AFe_2As_2 (A = Ba, Ca) revealed elastic anomalies that agree with a two-step process for the structural/magnetic transitions. Upon cooling, a pronounced velocity softening of longitudinal phonons propagating along the ***c*** axis is observed at the structural transition T_s due to a distortion of the lattice. Below a slightly lower temperature T_N, a biquadratic coupling between the distortion and an antiferromagnetic order parameter produces a steep velocity stiffening upon further cooling, the stiffening being five times larger in $CaFe_2As_2$ than in $BaFe_2As_2$. Microwave resistivity measurements at 16.5 GHz suggest that, upon cooling, the lattice distortion at T_s is driven by magnetic fluctuations in $BaFe_2As_2$, while it is rather due to lattice fluctuations in $CaFe_2As_2$. This suggestion appears consistent with a second-order character of the transitions in $BaFe_2As_2$ and a first-order one in $CaFe_2As_2$.

DOI: 10.1103/PhysRevB.89.155129 PACS number(s): 74.70.Xa, 72.55.+s, 63.20.kk, 62.65.+k

I. INTRODUCTION

The recent discovery of superconductivity in Fe-As-based materials has accelerated the search for new compounds constructed with the same building block, i.e., edge-shared $FeAs_4$ tetrahedron, in view of establishing a correlation between crystal structure, magnetism, and superconductivity. A common dynamic feature in pnictide families is the succession of two phase transitions. One is the structural phase transition at T_s from tetragonal at high temperatures to orthorhombic at low temperatures. The other is the long-range three-dimensional antiferromagnetic (AFM) spin density wave (SDW) order at T_N, with T_s slightly higher or equal to T_N [1]. Below $T_N \approx$ 130–220 K, a Fe^{2+} moment is aligned within the layer ***ab*** plane [1,2]. By introducing chemical doping (or hydrostatic pressure), both the structural and magnetic transitions are suppressed and superconductivity emerges above a critical concentration dependent on the substituent [3,4]. Since magnetism is considered as a common thread for the pairing interaction in unconventional superconductors, it is important to precise the microscopic origin of the AFM order [5]. For the iron pnictide families, consensus on the origin of the stripelike AFM order in the parent compounds is not yet established [2,6–8]. It may arise from the nesting between hole and electronlike Fermi pockets [9] or from localized moments consistent with the proximity of a Mott transition [10].

For the isostructural parent compounds $CaFe_2As_2$ and $BaFe_2As_2$, a nonmagnetic collapsed tetragonal phase appears under pressure [11], but, at ambient pressure, a lattice distortion from tetragonal to orthorhombic symmetry appears to be a requirement for AFM ordering, and its precise mechanism remains highly debated [12–19]. A strong softening of the C_{66} shear elastic constant is observed for $BaFe_2As_2$ [20,21] and explained by a renormalization by nematic fluctuations [20]. It was then concluded that the lattice softening was a secondary effect, with electronic degrees of freedom taking precedence over the elastic ones; the structural transition was then considered as a mere consequence of the magnetic ordering. Anomalous phonon behavior was also observed in Raman [22,23], infrared [24], and electron energy loss [25] spectroscopies; however it could not be explained by the orthorhombic distortion alone, because spin-phonon coupling has to be considered. Using inelastic neutron scattering, it was found that some phonons in $CaFe_2As_2$ showed a strong temperature dependence near the structural transition indicating a strong electron-phonon coupling and/or anharmonicity [26].

Beyond the apparent similarities of their magnetic and structural transitions, important differences are also observed between the $CaFe_2As_2$ and $BaFe_2As_2$ compounds. The combined structural-magnetic transition shows a first-order character in $CaFe_2As_2$ [27,28], when it looks predominantly second order in $BaFe_2As_2$ [29]. Moreover, although both compounds show a two-dimensional metallic character in the high temperature tetragonal phase, the electronic transport properties seem different in the orthorhombic one below T_s. For $BaFe_2As_2$, the in-plane resistivity shows a steep decrease at $T_s \approx$ 138 K and almost saturates below 75 K [30]. The resistivity shows rather a sharp increase at $T_s \approx$ 172 K for $CaFe_2As_2$ [31] before decreasing monotonically to low temperatures with a temperature profile that is practically identical to the high temperature metallic phase. A complex interrelation between charge, spin, and lattice degrees of freedom are clearly at the origin of the differences observed in the physical properties in the isostructural compounds $BaFe_2As_2$ and $CaFe_2As_2$.

To understand further the specifics of the combined structural and magnetic transition in $BaFe_2As_2$ and $CaFe_2As_2$, an investigation of the magnetoelastic coupling constitutes an appropriate route if one can have access independently to the spin and charge degrees of freedom on the same crystals. In this paper we address this issue by investigating the temperature dependence of a longitudinal compressional elastic modulus perpendicular to the ***ab*** plane with a pulsed ultrasonic technique. For both compounds, longitudinal

acoustic waves propagating along the ***c*** axis reveal well-defined anomalies in the temperature profile of the velocity that are associated with both structural and magnetic transitions at respectively T_s and T_N. Complementary microwave in-plane resistivity measurements, particularly sensitive to charge and spin degrees of freedom and performed on the same single crystals, provide a more precise understanding of the transition in this family of pnictides. On the one hand, a two-step process is established for *both* systems when the temperature is decreased, first the structural transition and then the magnetic one at a lower temperature; on the other hand, the predominant driving force appears to be different for the two compounds, spin fluctuations for $BaFe_2As_2$ and lattice ones for $CaFe_2As_2$.

II. EXPERIMENT

$BaFe_2As_2$ and $CaFe_2As_2$ single crystals were grown using the self-flux method [32] which yields platelike samples with the (001) direction perpendicular to the parallel shiny surfaces of the plate. The crystals had typical dimensions 2 mm × 1 mm × 0.1 mm. We use a pulsed ultrasonic interferometer to measure the variation of the longitudinal acoustic velocity along the crystal direction ***c*** relative to the value at $T_0 = 200$ K, $\Delta V/V = [V(T) - V(T_0)]/V(T_0)$. The acoustic pulses are generated with $LiNbO_3$ piezoelectric transducers resonating at 30 MHz and odd overtones bonded to the crystals with silicone seal. Since the high temperature crystal structure is tetragonal, the velocity is related to the C_{33} elastic constant or compressibility modulus through the relation $C_{33} = \rho V^2$, where ρ is the density. The ultrasonic technique is used in the transmission mode, and, because of the reduced thickness of the crystal along the ***c*** axis (∼0.1 mm), a CaF_2 delay line must be used to separate the first transmitted acoustic echo from the electric pulse. Moreover, no transverse acoustic mode can be properly analyzed because of mode conversion and mode mixing at the different interfaces. The longitudinal mode can be measured because it has the largest velocity that permits its time separation from parasitic signals. The $\Delta V/V$ data are directly the image of the relative variation of the compressibility modulus C_{33} if both the density and the sample's length changes can be neglected, an assumption that is generally verified in such materials. Variation of the attenuation $\Delta\alpha$ is obtained by monitoring the amplitude of the first transmitted acoustic pulse. The temperature was varied between 2 and 200 K.

The microwave resistivity is obtained on the exact same single crystals by using a standard cavity perturbation technique [33] operated in the TE_{102} mode at 16.5 GHz. Considering the in-plane resistivity value of the order of a few tenths mΩ cm [30], the electromagnetic field penetration is a few μm at this frequency, so we can treat the microwave data in the skin depth regime. To obtain the in-plane resistivity ρ_{ab}, the sample is either inserted in the cavity with the electric field parallel to the plate (E configuration) which induces currents in the ***ab*** plane, or with the magnetic field perpendicular to it along the ***c*** axis (H configuration), a configuration that induces also electric currents in the ***ab*** plane. Besides the charge degrees of freedom, the H configuration could also be sensitive to itinerant and/or localized spin preferentially oriented along the ***c*** axis. After insertion of the platelike crystal, we measure changes in the relative complex resonance frequency shift $[\Delta f/f + i\Delta(1/2Q)] = (\delta + i\Delta/2)$ (Q is the cavity quality factor) as a function of temperature. In the skin depth regime, the resistivity is proportional to $(\Delta/2)^2$ [34]. Because of large depolarization and demagnetization factors, absolute values are not very precise, and thus we consider only relative values $\rho_{ab}(T)/\rho_{ab}(180\text{ K})$. These microwave data will be compared with the direct current DC in-plane resistivity data obtained on other single crystals originating from the same growth batch which present temperature profiles similar to published data [30,31].

III. RESULTS

The ultrasonic velocity data are not dependent on frequency over the range 30–300 MHz for the two compounds investigated here. The attenuation generally increases with frequency due to the dissipation of the elastic waves by the crystal and the CaF_2 delay line, but the overall temperature profile remains frequency independent. Our ultrasonic and microwave results were not affected by an external magnetic field up to 18 tesla for any orientation relative to the crystal axes.

A. $BaFe_2As_2$

The ultrasonic data at 216 MHz are presented in Fig. 1 for the $BaFe_2As_2$ compound. When decreasing the temperature below 200 K, the velocity increases first monotonically in agreement with the stiffening of the interplane cohesion forces, saturates around 140 K, then decreases sharply near 136 K before increasing steeply to 80 K where it progressively recovers a monotonic increase toward low temperatures. These data agree with the overall temperature dependence previously reported for the C_{33} elastic constant [35], although no detailed investigation of the anomaly was conducted. Concomitantly the attenuation decreases smoothly below 200 K until a sharp peak is observed near 136 K before recovering the monotonic decrease to low temperatures. The elastic anomalies observed

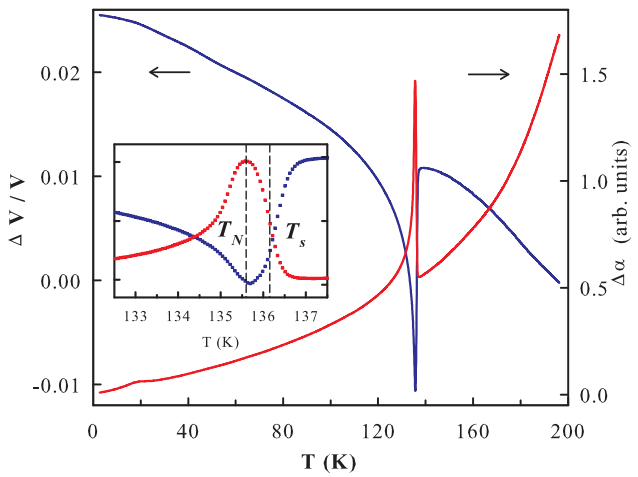

FIG. 1. (Color online) Temperature dependence of the variations of the longitudinal velocity $\Delta V/V$ and the attenuation $\Delta\alpha$ along the ***c*** axis below 200 K at 216 MHz for the $BaFe_2As_2$ compound. Inset: zoom of the elastic anomalies around 136 K; the dashed lines indicate the structural T_s and magnetic T_N transition temperatures.

near 136 K are clearly related to the structural-magnetic transitions. No thermal hysteresis could be detected consistently with a second order character of the transition.

The overall decrease of the attenuation from 200 to 2 K is dominated by the losses in the CaF_2 delay line, including the small slope variation below 20 K. Thus, the peak observed at the phase transition represents the main contribution of the $BaFe_2As_2$ crystal in the vicinity of the phase transition. When the high temperature wing of the peak is very abrupt, the low temperature one is much smoother and extends down to 80 K. The saturation of $\Delta V/V$ near 140 K signals a softening of the compression modulus C_{33} by magnetic and/or structural fluctuations. The steep decrease (∼2%) at 136 K cannot be attributed to the thermal expansivity along the $\boldsymbol{c}$ axis ($\Delta c/c$) which only amounts to ∼0.1% [36]. So, the velocity data translate an abrupt decrease of the C_{33} modulus at the phase transition. Below 136 K, the rapid increase of $\Delta V/V$ mimics the growth of a magnetic order parameter S_q obtained when a biquadratic coupling term between the order parameter S_q (at the wave vector $\mathbf{q}$) and the appropriate elastic strain $\mathbf{e}$ is considered [37]. The stiffening below 136 K amounts to 2.5%, a value similar to the former softening.

In the inset of Fig. 1 we show the temperature profile of the anomalies around 136 K. To differentiate the structural transition from the magnetic one, we show in Fig. 2(a) the temperature derivative of these anomalies where we can identify two features common to both sets of data at $T_N = 135.6(1)$ K and at $T_S = 136.2(1)$ K. On the one hand, the velocity stiffening below T_N coincides with maximum attenuation usually expected for magnetic transitions; on the other hand, the steep softening observed when approaching the transition from high temperatures shows a maximum rate (temperature derivative) at T_s where the attenuation increasing rate is also modified. These results suggest first a structural transition at T_s followed by a magnetic transition 0.5–0.6 K below. The nature of the fluctuations above T_s, magnetic and/or structural, remains to be determined. Going from T_s to T_N, the persistent softening of the velocity could be mainly due to three-dimensional fluctuations preceding the magnetic transition.

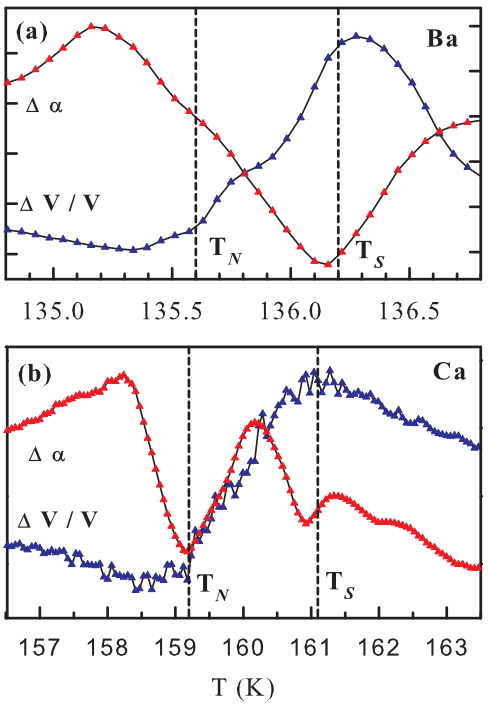

FIG. 2. (Color online) Temperature derivative of the velocity $\Delta V/V$ (blue) and the attenuation $\Delta\alpha$ (red) data at the phase transition: (a) $BaFe_2As_2$ and (b) $CaFe_2As_2$. The vertical dashed lines define the structural T_S and magnetic T_N transition temperatures.

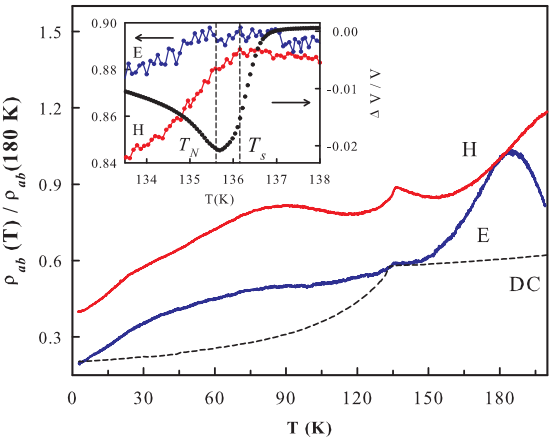

FIG. 3. (Color online) Temperature dependence of normalized in-plane resistivity $\rho_{ab}(T)/\rho_{ab}(180\text{ K})$ of $BaFe_2As_2$ below 200 K: microwave electric E field (blue) and magnetic H field (red) configurations. The DC curve was normalized to be coincident with the E field data. Inset: comparison of the microwave data (shifted vertically) with the ultrasonic velocity ones at the phase transition.

To push further the characterization of the transitions, we show in Fig. 3 the normalized in-plane microwave resistivity data $\rho_{ab}(T)/\rho_{ab}(180\text{ K})$ obtained for both microwave configurations. The temperature profile differs markedly from the DC resistivity which is also shown in Fig. 3 as a dashed line. For the electric field E configuration, the resistivity increases when the temperature is decreased below 200 K, goes through a maximum near 180 K, and decreases further below until it approaches 136 K where a small drop is observed. Instead of a saturation below 80 K, the resistivity decreases smoothly toward low temperatures. Below the transition at 136 K, the difference between the microwave and DC data could be explained by enhanced relaxation losses of the carriers in the low temperature metallic phase. Above the transition, in addition to relaxation effects, the dissipation peak at 180 K could be due to dielectric losses that cannot be observed in a DC experiment; their origin remains to be specified.

For the magnetic field H configuration, both the charge and spin degrees of freedom can contribute to the microwave losses. These additional spin contributions likely explain the difference observed with the E configuration and the DC curve in the vicinity of the phase transition. Indeed, the difference cannot be attributed to the anisotropy of in-plane resistivity which has been found independent of temperature [30]. Below 200 K, the normalized resistivity decreases smoothly, shows a local minimum around 160 K, and increases when approaching the phase transition. Below 136 K, the

H-field resistivity decreases by a larger amount compared with the E-field data but the temperature profile at low temperatures looks similar. Besides relaxation effects due to free carriers, the increase of the resistivity below 160 K is likely due to spin fluctuations preferentially along the ***c*** axis preceding the structural transition as reported in a neutron scattering experiment [38], a hypothesis consistent with the softening of the velocity below the same temperature (Fig. 1) when approaching T_s. This could signify that the spin degrees of freedom constitute the dominant driving force of the structural transition in this compound. In the inset of Fig. 3, we compare the microwave data to the elastic velocity ones at the phase transition. We clearly observe a correspondence between the values of T_s and T_N determined in the ultrasonic experiment, and well defined features on the microwave resistivity. The charge degrees of freedom are found insensitive to the structural transition and to magnetic fluctuations observed above T_s; only a weak decrease of resistivity is noticed below the magnetic transition T_N. On the contrary, the spins degrees of freedom are affected at both transitions: first a decrease at T_s and then a faster reduction (change of slope) when entering the magnetically ordered phase.

B. $CaFe_2As_2$

The ultrasonic data at 172 MHz are presented in Fig. 4 for the $CaFe_2As_2$ compound. While the general features observed are very similar to the former compound (Fig. 1), specific differences markedly distinguish the two systems. First, the elastic anomalies at the phase transition around 160 K are observed on a wider temperature range. Then, when decreasing the temperature below 200 K, $\Delta V/V$ presents a local maximum near 170 K before showing a sudden softening at the phase transition around 160 K. Finally, the stiffening below the transition is less steep, but its amplitude at low temperatures amounts to ≈12%, *practically five times larger* than $BaFe_2As_2$. Concomitantly the attenuation data present a peak centered at 160 K superposed on a rapidly increasing background at high temperatures due to the CaF_2 delay line. Thermal expansivity can contribute only 0.5% [36] to the softening of the velocity below 170 K. This implies that the amplitude of the softening at the phase transition is practically identical for both compounds and is likely due to a similar lattice distortion. The inset of Fig. 4 shows a zoom of the elastic anomalies around 160 K where we identify two maxima on $\Delta\alpha$. The temperature derivative of these anomalies shown in Fig. 2(b) suggests two transitions, corresponding approximately to the maximum temperature derivatives of $\Delta V/V$ indicated by dashed lines at $T_s = 161.1(1)$ K and $T_N = 159.2(1)$ K. As for $BaFe2As_2$ we have attributed the stiffening of $\Delta V/V$ below 160 K to the magnetic transition in agreement with a biquadratic coupling between the magnetic order parameter and the appropriate strain. So, when decreasing the temperature below 200 K, the structural transition precedes also the magnetic one for this system although the driving force appears different.

The microwave resistivity data $\rho_{ab}(T)/\rho_{ab}(180\text{ K})$ are shown in Fig. 5. For this compound the E and H configurations yield practically the same temperature dependence, which is an indication that charge degrees of freedom dominate over the spin ones especially for the H configuration. This is why there is a better similarity with the temperature profile of the DC resistivity, especially above the transition. Below 160 K, the local maximum near 90 K could also be due to enhanced carrier relaxation effects at microwave frequencies. The small maximum observed for the E-field configuration above 160 K could be related to relaxation and dielectric losses. For the H-field configuration, enhancement due to fluctuations is only observed in a narrow temperature range preceding the transition as shown in the inset of Fig. 5. Although AFM spin fluctuations were observed in this system [39], this result suggests that spin fluctuations along the ***c*** axis are much less important. Again there is an evident correlation between the transition temperatures T_s and T_N determined

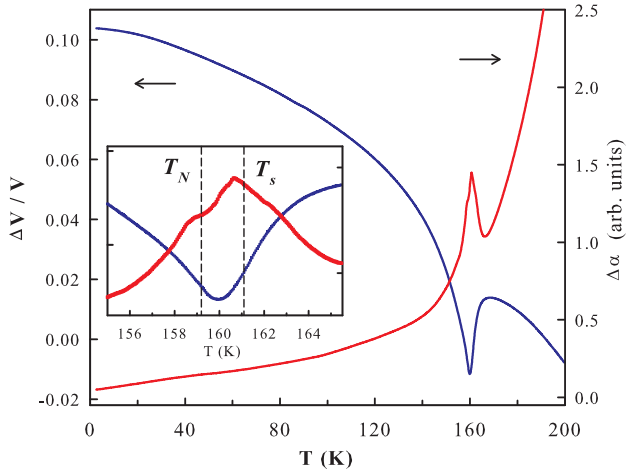

FIG. 4. (Color online) Temperature dependence of the variations of the longitudinal velocity $\Delta V/V$ and the attenuation $\Delta\alpha$ along the ***c*** axis below 200 K at 172 MHz for the $CaFe_2As_2$ compound. Inset: zoom of the elastic anomalies around 160 K; the dashed lines indicate the structural T_s and magnetic T_N transition temperatures.

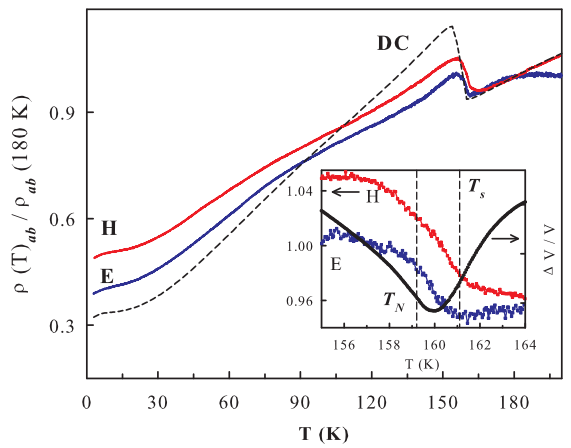

FIG. 5. (Color online) Temperature dependence of normalized in-plane resistivity $\rho_{ab}(T)/\rho_{ab}(180\text{ K})$ of $CaFe_2As_2$ below 200 K: microwave electric E field (blue) and magnetic H field (red) configurations. The DC curve was also normalized at 180 K. Inset: comparison of the microwave data with the ultrasonic velocity ones at the phase transition.

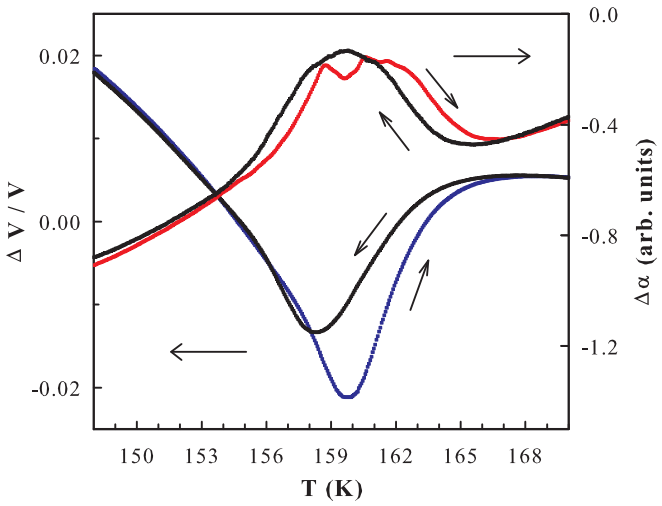

FIG. 6. (Color online) Thermal hysteresis on the elastic anomalies (243 MHz) at the phase transition in $CaFe_2As_2$. Arrows indicate the thermal cycling.

from the ultrasonic velocity data and features appearing on the microwave resistivity for both field configurations, increasing resistivity below $T_s = 161.1$ K [maximal temperature derivative of $\Delta V/V$, Fig. 2(b)] and variation of its increasing rate at $T_N = 159.2$ K [minimal temperature derivative of $\Delta V/V$, Fig. 2(b)]. Above the structural transition, although fluctuations have no effects on the charge degrees of freedom, an increase of resistivity (E field configuration) is detected at T_s with a subsequent slowing down at T_N with the progressive onset of the magnetic order. Except for spin fluctuation effects observed above T_s on the H field configuration, the temperature behavior of the two sets of data is very similar below T_s. The inset of Fig. 4 also suggests that the ultrasonic velocity softening observed below 170–180 K could be dominantly attributed to lattice fluctuations.

We show in Fig. 6 the thermal hysteresis cycle observed on the elastic anomalies at the phase transition in $CaFe_2As_2$ that confirms the first order character of both the structural and magnetic transitions. Upon cooling hysteretic effects begin to be observed below 170 K where a local maximum is observed on $\Delta V/V$. Such a wide temperature range is consistent with lattice fluctuations and domain wall formation that stabilizes the orthorhombic phase at T_s and subsequently the magnetic one at T_N. Upon warming the stabilized magnetic phase shifts to higher temperatures, pushing in turn the structural transition and strengthening the lattice distortion that softens the velocity at T_s. Although domains were observed upon cooling in $BaFe_2As_2$ and $CaFe_2As_2$ at the tetragonal to orthorhombic structural transition [40], domains could only be detected here in $CaFe_2As_2$ through hysteretic effects closely related to lattice fluctuations.

IV. DISCUSSION

The occurrence of an AFM ordered phase in these pnictides requires the breaking of the high-temperature phase via a lattice distortion from tetragonal to orthorhombic symmetry, a distortion that is expected to yield a softening of the acoustic phonon modes when passing the structural transition. This has indeed been observed for a transverse acoustic phonon in $BaFe_2As_2$ [41]. The important softening of the longitudinal acoustic phonons propagating along the ***c*** axis observed in our ultrasonic experiments at the structural transition is clearly due to a sudden lattice distortion in both compounds. Although the thermal expansion coefficients differ for the two compounds [36], the distortion produces an almost identical softening of the C_{33} modulus.

For $BaFe_2As_2$ it has been shown that the structural/magnetic transitions are described by a two-step process [29]: a second-order structural transition from the high-temperature paramagnetic tetragonal structure to a paramagnetic orthorhombic phase followed by a discontinuous step in the structural order parameter coincident with a first-order AFM transition. Simultaneous first-order transitions were instead found in $CaFe_2As_2$ [42]. Our ultrasonic and microwave data definitely confirm a two-step process for both compounds when decreasing the temperature: First there is a structural transition at T_s when a spontaneous orthorhombic lattice distortion produces a sudden velocity softening and an increase of the attenuation; subsequently, in the orthorhombic phase, the longitudinal lattice strain couples to the magnetic order parameter at T_N to yield an increase of the velocity which mimics the rapid growth of the order parameter below T_N. At much lower temperatures, when the AFM order parameter has reached its maximum value, the velocity recovers its usual anharmonic behavior. Attenuation peaks are expected at both transitions and are indeed observed for $BaFe_2As_2$ due to a 2 K temperature separation; for $CaFe_2As_2$, a separation of only 0.6 K renders the observation of the two peaks more difficult. If the transitions are characterized first order in $CaFe_2As_2$, no first-order behavior could be identified in $BaFe_2As_2$ at either transitions.

A mechanism of electron-phonon coupling has been suggested to describe the interaction between the lattice softening and the onset of magnetic ordering in these compounds [29,41,42]. More specifically a biquadratic coupling between the structural and magnetic order parameters was inferred in $BaFe_2As_2$ [43]. Our results clearly confirm that a biquadratic coupling term is indeed appropriate to render account of the rapid stiffening of the velocity in the two compounds. However, the coupling is much larger for $CaFe_2As_2$; an explanation for this is likely related to the first-order character of the transition and to the precise driving force leading to the lattice distortion.

Our microwave resistivity data suggest some trails to precise the driving mechanism. In $BaFe_2As_2$ magnetic fluctuations are observed approximately 30 K above $T_s = 136.1$ K (Fig. 3) resulting in a velocity softening preceding the structural transition. The steepness of the softening at T_s indicates that the lattice fluctuations are restricted over a narrow temperature range (less than 1 K). The spin degrees of freedom then constitute the main driving force of the lattice distortion. This has to be compared to the spin-Peierls second-order phase transition in quasi-one-dimensional systems where spins induce a distortion of the lattice. In $CaFe_2As_2$ however, the situation is inverted: Spin fluctuations are restricted to a narrow temperature range above $T_s = 161.1$ K (Fig. 5) when the softening of the velocity extends more than 20 K

above (Fig. 4). For this system, the driving force of the lattice distortion comes predominantly from the lattice fluctuations, an assumption which is consistent with the first-order character of the transition and the observation of hysteretic effects.

V. CONCLUSION

Pulsed ultrasonic experiments performed on thin pnictide single crystals $CaFe_2As_2$ and $BaFe_2As_2$ have confirmed that a two-step process is involved in the structural/magnetic transitions. Upon cooling, a pronounced softening of an acoustic longitudinal phonon at the structural transition T_s is observed for both systems with similar amplitudes. The magnetic transition follows at T_N, respectively, 0.5 K and 1.9 K below T_s for $BaFe_2As_2$ and $CaFe_2As_2$. The onset of magnetic ordering results from a biquadratic coupling between the structural and magnetic order parameters, which is approximately five times stronger for $CaFe_2As_2$. Such a difference between the two systems appears to be related to the nature of the transitions, first-order for $CaFe_2As_2$ and second-order for $BaFe_2As_2$, and to the driving mechanism leading to the lattice distortion. Our microwave resistivity data using the H component of the electromagnetic field have unveiled that spin fluctuations dominate the approach of the structural transition in $BaFe_2As_2$ consistently with the second-order character of the transition, when they are almost absent for $CaFe_2As_2$. In the latter system, lattice fluctuations and domain wall formation are responsible for the softening of the velocity when approaching T_s upon cooling, and they constitute the main driving force for the first-order structural transition.

ACKNOWLEDGMENTS

The authors acknowledge the technical support of Mario Castonguay. This work was supported by grants from the Fonds Québécois de la Recherche sur la Nature et les Technologies (FQRNT), the Natural Science and Engineering Research Council of Canada (NSERC), and US NSF through DMR-1002622.

[1] For a review, see M. D. Lumsden and A. D. Christianson, J. Phys.: Condens. Matter **22**, 203203 (2010).
[2] Q. Huang, Y. Qiu, W. Bao, M. A. Green, J. W. Lynn, Y. C. Gasparovic, T. Wu, G. Wu, and X. H. Chen, Phys. Rev. Lett. **101**, 257003 (2008).
[3] N. Ni, A. Thaler, J. Q. Yan, A. Kracher, E. Colombier, S. L. Bud'ko, P. C. Canfield, and S. T. Hannahs, Phys. Rev. B **82**, 024519 (2010).
[4] A. P. Dioguardi, N. apRoberts-Warren, A. C. Shockley, S. L. Bud'ko, N. Ni, P. C. Canfield, and N. J. Curro, Phys. Rev. B **82**, 140411(R) (2010).
[5] D. J. Scalapino, Rev. Mod. Phys. **78**, 17 (2012).
[6] C. de la Cruz, Q. Huang, J. W. Lynn, J. Li, W. R. Ii, J. L. Zaretsky, H. A. Mook, G. F. Chen, J. L. Luo, N. L. Wang, and P. Dai, Nature (London) **453**, 899 (2008).
[7] J. Zhao, D. T. Adroja, D.-X. Yao, R. Bewley, S. Li, X. F. Wang, G. Wu, X. H. Chen, J. Hu, and P. Dai, Nat. Phys. **5**, 555 (2009).
[8] H. Luetkens, H. H. Klauss, M. Kraken, F. J. Litterst, T. Dellmann, R. Klingeler, C. Hess, R. Khasanov, A. Amato, C. Baines, M. Kosmala, O. J. Schumann, M. Braden, J. Hamann-Borrero, N. Leps, A. Kondrat, G. Behr, J. Werner, and B. Buchner, Nat. Mater. **8**, 305 (2009).
[9] P. J. Hirschfeld, M. M. Korshunov, and I. I. Mazin, Rep. Prog. Phys. **74**, 124508 (2011).
[10] D. N. Basov and A. V. Chubukov, Nat. Phys. **7**, 272 (2011).
[11] A. Kreyssig, M. A. Green, Y. Lee, G. D. Samolyuk, P. Zajdel, J. W. Lynn, S. L. Bud'ko, M. S. Torikachvili, N. Ni, S. Nandi, J. B. Leão, S. J. Poulton, D. N. Argyriou, B. N. Harmon, R. J. McQueeney, P. C. Canfield, and A. I. Goldman, Phys. Rev. B **78**, 184517 (2008).
[12] H. Kontani, T. Saito, and S. Onari, Phys. Rev. B **84**, 024528 (2011).
[13] T. Goto, R. Kurihara, K. Araki, K. Mitsumoto, M. Akatsu, Y. Nemoto, S. Tatematsu, and M. Sato, J. Phys. Soc. Jpn. **80**, 073702 (2011).
[14] I. Paul, Phys. Rev. Lett. **107**, 047004 (2011).
[15] M. D. Johannes, I. I. Mazin, and D. S. Parker, Phys. Rev. B **82**, 024527 (2010).
[16] M. D. Johannes and I. I. Mazin, Phys. Rev. B **79**, 220510 (2009).
[17] T. Yildirim, Physica C **469**, 425 (2009).
[18] C.-C. Lee, W.-G. Yin, and W. Ku, Phys. Rev. Lett. **103**, 267001 (2009).
[19] H. Kontani and S. Onari, Phys. Rev. Lett. **104**, 157001 (2010).
[20] R. M. Fernandes, L. H. VanBebber, S. Bhattacharya, P. Chandra, V. Keppens, D. Mandrus, M. A. McGuire, B. C. Sales, A. S. Sefat, and J. Schmalian, Phys. Rev. Lett. **105**, 157003 (2010).
[21] M. Yoshizawa, D. Kimura, T. Chiba, S. Simayi, Y. Nakanishi, K. Kihou, C.-H. Lee, A. Iyo, H. Eisaki, M. Nakajima, and S.-i. Uchida, J. Phys. Soc. Jpn. **81**, 024604 (2012).
[22] L. Chauviere, Y. Gallais, M. Cazayous, A. Sacuto, M. A. Méasson, D. Colson, and A. Forget, Phys. Rev. B **80**, 094504 (2009).
[23] M. Rahlenbeck, G. L. Sun, D. L. Sun, C. T. Lin, B. Keimer, and C. Ulrich, Phys. Rev. B **80**, 064509 (2009).
[24] A. A. Schafgans, B. C. Pursley, A. D. LaForge, A. S. Sefat, D. Mandrus, and D. N. Basov, Phys. Rev. B **84**, 052501 (2011).
[25] J. Teng, C. Chen, Y. Xiong, J. Zhang, R. Jin, and E. W. Plummer, Proc. Natl. Acad. Sci. USA **110**, 898 (2013).
[26] R. Mittal, L. Pintschovius, D. Lamago, R. Heid, K.-P. Bohnen, D. Reznik, S. L. Chaplot, Y. Su, N. Kumar, S. K. Dhar, A. Thamizhavel, and Th. Brueckel, Phys. Rev. Lett. **102**, 217001 (2009).
[27] N. Ni, S. Nandi, A. Kreyssig, A. I. Goldman, E. D. Mun, S. L. Bud'ko, and P. C. Canfield, Phys. Rev. B **78**, 014523 (2008).
[28] K.-Y. Choi, D. Wulferding, P. Lemmens, N. Ni, S. L. Bud'ko, and P. C. Canfield, Phys. Rev. B **78**, 212503 (2008).
[29] M. G. Kim, R. M. Fernandes, A. Kreyssig, J. W. Kim, A. Thaler, S. L. Bud'ko, P. C. Canfield, R. J. McQueeney, J. Schmalian, and A. I. Goldman, Phys. Rev. B **83**, 134522 (2011).
[30] X. F. Wang, T. Wu, G. Wu, H. Chen, Y. L. Xie, J. J. Ying, Y. J. Yan, R. H. Liu, and X. H. Chen, Phys. Rev. Lett. **102**, 117005 (2009).

[31] F. Ronning, T. Klimczuk, E. D. Bauer, H. Volz, and J. D. Thompson, J. Phys.: Condens. Matter **20**, 322201 (2008).
[32] A. S. Sefat, R. Jin, M. A. McGuire, B. C. Sales, D. J. Singh, and D. Mandrus, Phys. Rev. Lett. **101**, 117004(E) (2008).
[33] L. Buravov and J. F. Shchegolev, Prib. Tekh. Eksp. **2**, 171 (1971).
[34] N. P. Ong, J. Appl. Phys. **48**, 2935 (1977).
[35] S. Simayi, K. Sakano, H. Takezawa, M. Nakamura, Y. Nakanishi, K. Kihou, M. Nakajima, C.-H. Lee, A. Iyo, H. Eisaki, S.-i. Uchida, and M. Yoshizawa, J. Phys. Soc. Jpn. **82**, 114604 (2013).
[36] S. L. Bud'ko, N. Ni, and P. C. Canfield, Phil. Mag. **90**, 1219 (2010).
[37] J. Pouget, in *Low-Dimensional Elctronic Properties of Molybdenum Bronzes and Oxides*, edited by C. Schlenker (Kluwer Academic, Netherlands, 1989), pp. 87–157.
[38] C. Wang, R. Zhang, F. Wang, H. Luo, L. P. Regnault, P. Dai, and Y. Li, Phys. Rev. X **3**, 041036 (2013).
[39] D. K. Pratt, Y. Zhao, S. A. J. Kimber, A. Hiess, D. N. Argyriou, C. Broholm, A. Kreyssig, S. Nandi, S. L. Bud'ko, N. Ni, P. C. Canfield, R. J. McQueeney, and A. I. Goldman, Phys. Rev. B **79**, 060510(R) (2009).
[40] M. A. Tanatar, A. Kreyssig, S. Nandi, N. Ni, S. L. Bud'ko, P. C. Canfield, A. I. Goldman, and R. Prozorov, Phys. Rev. B **79**, 180508(R) (2009).
[41] J. L. Niedziela, D. Parshall, K. A. Lokshin, A. S. Sefat, A. Alatas, and T. Egami, Phys. Rev. B **84**, 224305 (2011).
[42] A. I. Goldman, D. N. Argyriou, B. Ouladdiaf, T. Chatterji, A. Kreyssig, S. Nandi, N. Ni, S. L. Bud'ko, P. C. Canfield, and R. J. McQueeney, Phys. Rev. B **78**, 100506(R) (2008).
[43] S. D. Wilson, Z. Yamani, C. R. Rotundu, B. Freelon, E. Bourret-Courchesne, and R. J. Birgeneau, Phys. Rev. B **79**, 184519 (2009).